

## Electronic Supplementary Information

# Discovering Positively Charged Pt for Enhanced Hydrogenolysis of Glycerol to 1,3-Propanediol

Binbin Zhao<sup>a</sup>, Yu Liang<sup>a</sup>, Lei Liu<sup>a\*</sup>, Qian He<sup>b\*</sup> and Jinxiang Dong<sup>a,c</sup>

<sup>a</sup>College of Chemistry and Chemical Engineering, Taiyuan University of Technology, Taiyuan, Shanxi030024, P. R. China. E-mail: liulei@tyut.edu.cn

<sup>b</sup>Department of Materials Science and Engineering, National University of Singapore, Singapore 117575. E-mail: heqian@nus.edu.sg

<sup>c</sup>School of Chemical Engineering and Light Industry, Guangdong University of Technology, Guangzhou 510006, P. R. China.

### Contents

#### 1. Experimental Procedures

- Chemicals
- Synthesis of  $T\text{-Ta}_2\text{O}_5$
- Synthesis of  $\text{WO}_x/T\text{-Ta}_2\text{O}_5$
- Synthesis of  $\text{Pt}^{\delta+}/T\text{-Ta}_2\text{O}_5$  and  $\text{Pt}^{\delta+}/\text{WO}_x/T\text{-Ta}_2\text{O}_5$
- Synthesis of  $\text{Pt}^0/\text{WO}_x/T\text{-Ta}_2\text{O}_5$
- Catalyst Characterization
- Catalytic Reactions

#### 2. Results and Discussion

- Supporting Figures S1-S12
- Supporting Tables S1-S4

#### 3. References

## 1. Experimental procedure

### Chemicals

Tantalum chloride anhydrous ( $\text{TaCl}_5$ , 99.99%, metals basis) was purchased from J&K. Potassium hydroxide (KOH, 99.99% metals basis), chloroplatinic acid hexahydrate ( $\text{H}_2\text{PtCl}_6 \cdot 6\text{H}_2\text{O}$ , AR, Pt  $\geq 37.5\%$ ), ammonium metatungstate ( $(\text{NH}_4)_6\text{H}_2\text{W}_{12}\text{O}_{40} \cdot x\text{H}_2\text{O}$ , 99.5% metals basis), ethanol ( $\text{CH}_3\text{CH}_2\text{OH}$ ,  $\geq 99.5\%$ , moisture  $\leq 0.005\%$ ) and glycerol (ACS,  $\geq 99.5\%$ ) were purchased from Aladdin.

### Synthesis of $T\text{-Ta}_2\text{O}_5$

$\text{Ta}_2\text{O}_5$  was prepared according to the method previously reported in the literature.<sup>1</sup> Typically,  $\text{TaCl}_5$  was hydrolyzed with KOH in ethanol. Namely, 2.6 g KOH and 2.5 g  $\text{TaCl}_5$  were dissolved in 15 mL ethanol, respectively, and stirred at room temperature for 3h. Then, KOH solution was added drop wise to  $\text{TaCl}_5$  solution and stirred 14h at room temperature. After aging the precipitate at 40 °C in an oven for 24 h, the precipitate was suspended into boiling 1 M HCl aqueous solution for 1h. The obtained precipitate was suspended into the boiling distilled water for 1 h for washing. This process was repeated until chloride ions were not detected. The obtained solid was dried at 110 °C for 12 h and calcined at 900 °C (2 °C /min) for 3h in a muffle furnace, and the final obtained tantalum oxide was denoted as  $T\text{-Ta}_2\text{O}_5$ .

### Synthesis of $\text{WO}_x/T\text{-Ta}_2\text{O}_5$

The typical  $\text{WO}_x/T\text{-Ta}_2\text{O}_5$  was prepared as follows: firstly, 0.3367g of ammonium metatungstate ( $(\text{NH}_4)_6(\text{H}_2\text{W}_{12}\text{O}_{40}) \cdot n\text{H}_2\text{O}$ ) was dissolved in deionized water, and 5 g of  $T\text{-Ta}_2\text{O}_5$  was added in the solution with stirring for 24 h at room temperature. Then, the solid samples were centrifuged, dried at 110 °C in an oven for 12 h, and calcined at 500 °C for 3h in air in a muffle furnace. The final  $\text{WO}_x/T\text{-Ta}_2\text{O}_5$  sample was used for loading Pt.

### Synthesis of $\text{Pt}^{\delta+}/T\text{-Ta}_2\text{O}_5$ and $\text{Pt}^{\delta+}/\text{WO}_x/T\text{-Ta}_2\text{O}_5$

The platinum was supported on  $T\text{-Ta}_2\text{O}_5$  and  $\text{WO}_x/T\text{-Ta}_2\text{O}_5$  by impregnation method, respectively. Firstly, the required amount of chloroplatinic acid ( $\text{H}_2\text{PtCl}_6 \cdot 6\text{H}_2\text{O}$ ) was added to 40 mL of distilled water in a beaker and stirred at room temperature. Subsequently, 2 g of  $\text{Ta}_2\text{O}_5$  or  $\text{WO}_x/T\text{-Ta}_2\text{O}_5$  was added with stirring for 24 h at room temperature, followed by evaporation to remove the water at 110 °C in an oven for 12 h. The obtained solid was crushed to a fine powder and calcined at 300 °C for 3 h in a muffle furnace to obtain  $\text{Pt}^{\delta+}/T\text{-Ta}_2\text{O}_5$  or  $\text{Pt}^{\delta+}/\text{WO}_x/T\text{-Ta}_2\text{O}_5$  catalysts.

### Synthesis of $\text{Pt}^0/\text{WO}_x/T\text{-Ta}_2\text{O}_5$

For comparison,  $\text{Pt}^0/\text{WO}_x/T\text{-Ta}_2\text{O}_5$  was prepared by reducing  $\text{Pt}^{\delta+}/\text{WO}_x/T\text{-Ta}_2\text{O}_5$  sample in flowing 10%  $\text{H}_2/\text{Ar}$  (120 ml/min) at 300 °C for 3 h.

### Catalyst Characterization

The X-ray diffraction (XRD) patterns were recorded with a D8 Bruker employing Cu-K $\alpha$  radiation monochromatized radiation ( $\lambda = 0.1541$  nm) operated at 40 kV and 40 mA. The  $2\theta$  range from 15° to 80° with 0.02° step were recorded at a scanning rate of 4° /min.

Nitrogen adsorption–desorption isotherms were obtained on a Micromeritics ASAP 2020 instrument at 77K. The samples were degassed at 200 °C for 10 h, and then Brunauer–Emmett–Teller (BET) method was used to calculate the specific surface areas ( $S_{\text{BET}}$ ).

Metal content in the catalyst was determined by inductively coupled plasma atomic emission spectroscopy (ICP-AES, Thermo iCAP6300).

Raman spectra were measured using a Renishaw in-Via Reflex micro-Raman spectrometer in the back-scattering geometry. The samples excitation was carried out by using a 532 nm emission line of a DPSS laser, and the scattered light was collected through a 50× objective lens. The spectral resolution was approximately  $1\text{ cm}^{-1}$ . The duration of exposure and number of accumulation was set as 3s and 3 times, respectively.

The UV-Vis absorption spectra were recorded on a Perkin-Elmer Lambda 750 UV/Vis/NIR Spectrometer from 200 to 700 nm with a step size of 1 nm. BaSO<sub>4</sub> was used as a standard reflector.

Scanning electron microscopy (SEM) images were recorded on a Hitachi SEM (SU8010, Hitachi, Japan) equipped with a Horiba X-Max 50 EDX system. The samples were attached to a double-sided carbon conductive adhesive tape on an aluminum slab and coated with gold.

High angle annular dark field scanning transmission electron microscopy (HAADF-STEM) were carried out using an aberration-corrected JEOL ARM200CF microscope operated at 200 kV.

FT-IR spectra for CO adsorption on the two samples were collected at 40 °C with a Bruker INVENIO R spectrometer equipped with a LN-MCT Mid detector at a resolution of  $4\text{ cm}^{-1}$  using 16 scans for all sample. Before CO adsorption, the samples were pretreated in pure Ar (30 mL/min) at 300 °C for 1h to clean the surface from moisture. Then cooling to 40 °C and purged with pure Ar for 30 min, background spectra were taken at 40 °C for the spectra measured post-adsorption spectra. After change the gas flow to 10%CO/He continued for 30 min, the DRIFTS spectra were recorded till no visible change in the absorption band intensities under Ar purging.

Temperature programmed desorption of NH<sub>3</sub> (NH<sub>3</sub>-TPD) and temperature programmed reduction (TPR) analysis were performed on a Micromeritics AutoChem II 2920. For NH<sub>3</sub>-TPD, 50 mg of catalyst was pretreated in He at 400 °C for 1 h to clean the surface from moisture and other adsorbed gases. After cooling to 100 °C, the catalyst was saturated with 5% NH<sub>3</sub>/He gas mixtures for 2 h and then purged with He to remove the physisorbed NH<sub>3</sub> for 1 h. Subsequently, the sample was heated to 700 °C at a ramp rate of 10 °C /min and the NH<sub>3</sub> desorption was detected by a thermal conductivity detector (TCD). For TPR analysis, 50 mg of catalyst was pretreated in Ar at 300 °C for 1h. And then cooling to 40 °C, 10% H<sub>2</sub>/90% Ar gas mixtures was introduced into the system and a cold trap of 2-propanol liquid nitrogen slurry was provided to condense the water gas. The sample was heated to 900 °C at a ramp rate of 10 °C /min and recorded by a thermal conductivity detector.

For H<sub>2</sub>-O<sub>2</sub> titration analysis was performed on a Micromeritics AutoChem II 2920. Firstly, 50mg of catalysts (Pt<sup>δ+</sup>/WO<sub>x</sub>/T-Ta<sub>2</sub>O<sub>5</sub>-Air, Pt/T-Ta<sub>2</sub>O<sub>5</sub>-Air, Pt<sup>δ+</sup>/WO<sub>x</sub>/T-Ta<sub>2</sub>O<sub>5</sub>-H<sub>2</sub>, WO<sub>x</sub>/T-Ta<sub>2</sub>O<sub>5</sub>-Air) was pre-treated at 300 °C with flowing pure Ar for 1 h to remove the moisture absorbed on catalyst. After that, it was cooling to 100 °C and purging with Air for 30 min, and then purged with Ar again for 30 min to remove the oxygen absorbed on Pt atoms. Finally, Argon was used as carried gas at 50 mL min<sup>-1</sup>, and the successive doses of 5%H<sub>2</sub>/Ar gas were subsequently introduced into Ar stream by means of a calibrated injection valve (483 μL 5% H<sub>2</sub>/Ar pulse<sup>-1</sup>) at 100 °C. The titration will end until the intensities of peaks in a row keeps constant.

FT-IR spectra after pyridine adsorption (Py-IR) were obtained using a Bruker INVENIO R spectrometer equipped with a DTGS detector. The catalyst was pressed into self-supporting wafers and degassed in vacuum at 300 °C for 1 h. After that, it was cooled down to 40 °C and followed by exposure to pyridine vapor. The Py-IR spectrum was recorded at 100 °C and 300 °C after evacuation for 30min.

X-ray photoelectron spectroscopy (XPS) was measured on an AXIS ULTRA DLD spectrometer with Al K $\alpha$  resource ( $h\nu = 1486.6\text{ eV}$ ). The base pressure in the measurement chamber was maintained under high vacuum conditions. The contaminated carbon C 1s signal at 284.8 eV was used to calibrate binding energies. The XPS PEAK41 software was used to analyze the XPS data.

### Catalytic reactions

The hydrogenolysis of glycerol was carried out in a 25 mL-capacity Teflon-lined stainless steel autoclave. 200 mg of catalyst and 6.184g of 3 wt% (or 30 wt %) glycerol aqueous solution were added to the Teflon-lined. And then the autoclave was sealed and purged with H<sub>2</sub> six times to expel air. During the reaction, the temperature was maintained at 160 °C, the H<sub>2</sub> pressure was 5.0 MPa, and the stirring rate was 600 rpm. After rising to the target pressure, hydrogen is added during the reaction to keep the target pressure unchanged. After the reaction, the liquid phase was analyzed by an HPLC (Shimadzu, LC-20AD) equipped with a RID detector. The column used was a 4.6×250 mm C18 column with the filler size of 5 μm (Inertsil ODS-3, Catalog No.5020-01732). The column was run using a mobile phase of Milli-Q water at a flow rate of 0.5 mL/min at 35 °C. The amounts of consumed glycerol and produced products were quantified with an external calibration method. TOF was acquired at glycerol conversion of 4.8%. The standard deviation for the product quantitative analysis was within 0.5%.

The hydrogenation of propanal to 1-PrOH was out in a 25 mL Teflon-lined stainless steel autoclave. 50 mg of catalyst and 6 g of 3 wt% propanal aqueous solution were added to the autoclave. And then the autoclave was sealed and purged with H<sub>2</sub> six times to expel air. During the reaction, the temperature was maintained at 25 °C, the H<sub>2</sub> pressure was 2.0 MPa, and the stirring rate was 600 rpm. The liquid product was analyzed by off-line gas chromatography (shimadzu, GC-2010 Pro) using a FID detector and a Wonda Cap-WAX capillary column (0.32 mm×30 m×0.25 μm).

The conversion of glycerol and the selectivity of the liquid product were calculated by the following equations.

$$\text{Conversion (\%)} = (\text{moles of glycerol converted}) \times 100\% / (\text{initial moles of glycerol})$$

$$\text{Selectivity (\%)} = (\text{carbon moles of one specific product}) \times 100\% / (\text{all the carbon moles in glycerol converted})$$

The turnover frequency (TOF) of 1,3-PDO at conversion less than 10% was calculated as follows:

$$\text{TOF} = (\text{moles of glycerol converted} \times S_{1,3\text{-PDO}} \times M_{1,3\text{-PDO}}) / (\text{catalyst weight} \times \text{Pt loading} \times \text{reaction time})$$

## 2. Results and Discussion

**Table S1.** The results of different catalyst in hydrogenolysis of glycerol.

Catalyst	Pt Loading (wt%)	W/WO <sub>3</sub> Loading (wt%)	Conversion %	Sel		TOF <sub>1,3-PDO</sub> g g <sub>Pt</sub> <sup>-1</sup> h <sup>-1</sup>	Sel (%) (1,3/1,2)	Reference
				1,3-PDO	1,2-PDO			
Pt/WO <sub>x</sub> /Al <sub>2</sub> O <sub>3</sub>	9	8	53.1	51.9	9.5	-	5.5	2
Pt/WO <sub>3</sub> /SBA-15	2	10	86.0	42	11.0	15.2	3.8	3
Pt/WO <sub>x</sub> /γ-Al <sub>2</sub> O <sub>3</sub>	2	10	64.2	66.1	5.7	1.6	11.6	4
Pt/WO <sub>x</sub> /AlOOH	2	8	100.0	66	2.0	-	33.0	5
Pt/WO <sub>3</sub> /ZrO <sub>2</sub>	2	20	85.8	28.21	14.57	-	1.9	6
Pt/WO <sub>3</sub> /SiO <sub>2</sub> /ZrO <sub>2</sub>	2	15	54.3	52	6.8	1.2	7.7	7
Pt/WO <sub>3</sub> /TiO <sub>2</sub> /SiO <sub>2</sub>	2	5	15.3	50.5	9.2	-	5.5	8
Pt/WO <sub>x</sub> /t-ZrO <sub>2</sub>	1.94	7.56	78.3	64.8	1.6	5.1	40.5	9
2W4Pt/SiO <sub>2</sub>	4	2	64.2	57.2	10.5	-	5.45	10
Pt/WO <sub>x</sub> /γ-Al <sub>2</sub> O <sub>3</sub>	6	12.9	80.4	35.3	4.9	3.2	7.2	11
This work	0.68	0.51	87.00	45.61	0.76	30.80	63.96	-

**Table S2.** The essential physicochemical properties of the as-synthesized catalyst.

Sample	S <sub>BET</sub>	Pt Loading (wt%)	W Loading (wt%)
T-Ta <sub>2</sub> O <sub>5</sub>	10.38	/	/
Pt <sup>δ+</sup> /T-Ta <sub>2</sub> O <sub>5</sub>	10.65	0.70	/
Pt <sup>δ+</sup> /WO <sub>x</sub> /T-Ta <sub>2</sub> O <sub>5</sub>	9.46	0.68	0.51

**Table S3.** The catalytic results of glycerol hydrogenolysis with different reaction times over Pt<sup>δ+</sup>WO<sub>x</sub>/T-Ta<sub>2</sub>O<sub>5</sub>

Catalyst	Time h	Conversion (%)	sel. (%) 1,3-PDO	sel. (%)				Y <sub>1,3-PDO</sub> Sel	(S <sub>1,3/1,2</sub> )
				1,2-PDO	2-PrOH	1-PrOH	Others		
Pt <sup>δ+</sup> /WO <sub>x</sub> /T-Ta <sub>2</sub> O <sub>5</sub>	1	18.64	48	2.89	6.31	41.2	1.6	8.95	16.61
	2	33.21	45.52	2.33	5.39	43.8	2.95	15.08	19.5
	4	50.22	45.92	2	4.64	45.96	1.48	23.06	22.96
	6	67.05	44.13	1.28	4.63	44.84	5.12	29.59	34.48
	8	77.93	42.43	1.06	4.38	45.34	6.79	33.06	40.18
	12	89.88	44.80	0.65	4.42	42.36	7.77	40.26	68.61

Reaction conditions: 200 mg of catalyst, 6.184 g of 3 wt% glycerol aqueous solution, temperature 160 °C, H<sub>2</sub> pressure of 5.0 MPa, stirring rate of 600 rpm.

**Table S4.** XPS fitting results for the fresh catalyst, as well as the spent catalysts after the first run and the fourth run.

Catalyst	Pt 4f <sub>7/2</sub> BE (eV)		Pt <sup>δ+</sup> /(Pt <sup>δ+</sup> + Pt <sup>0</sup> )
	Pt <sup>δ+</sup>	Pt <sup>0</sup>	
Pt <sup>δ+</sup> /WO <sub>x</sub> /T-Ta <sub>2</sub> O <sub>5</sub>	72.95	-	100%
Pt <sup>δ+</sup> /WO <sub>x</sub> /T-Ta <sub>2</sub> O <sub>5</sub> -1st	72.8	71.18	54.95%
Pt <sup>δ+</sup> /WO <sub>x</sub> /T-Ta <sub>2</sub> O <sub>5</sub> -4th	72.7	71.22	44.26%

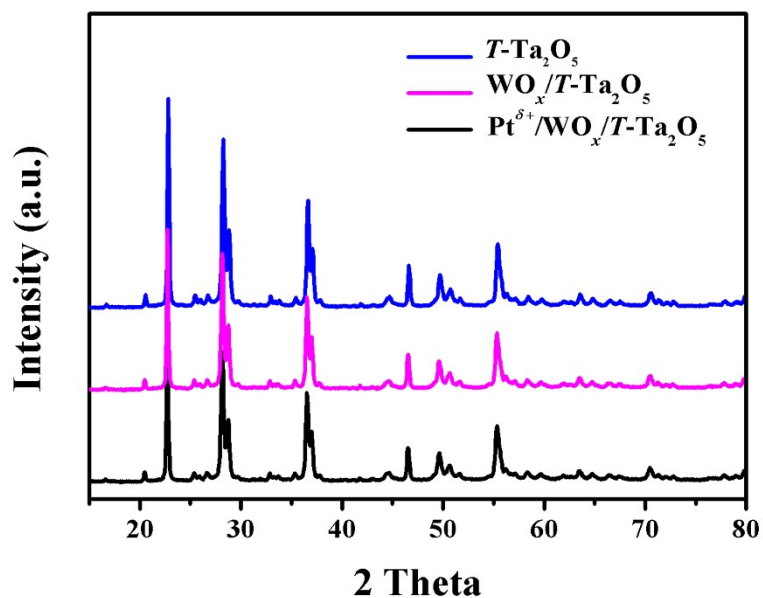
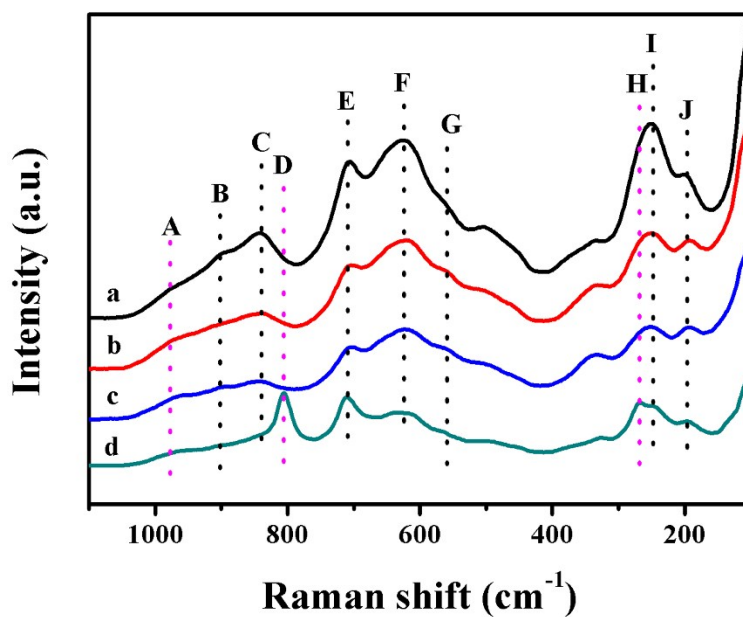


Figure S 1. Powder XRD patterns of the catalysts.



**Figure S 2.** Raman spectra of the  $T\text{-Ta}_2\text{O}_5$  (a),  $\text{WO}_x/T\text{-Ta}_2\text{O}_5$  (b),  $\text{Pt}^{\delta+}/\text{WO}_x/T\text{-Ta}_2\text{O}_5$  (c) 5% $\text{WO}_x/T\text{-Ta}_2\text{O}_5$  (d) catalysts. The origin of weak peak B around at  $900\text{ cm}^{-1}$  is due to variation in bond lengths. The other band C at  $845\text{ cm}^{-1}$  is signed for  $\text{TaO}_7$  in  $\beta\text{-Ta}_2\text{O}_5$ . The Raman bands for E, F and G correspond to symmetric O–Ta vibrations in  $\text{TaO}_6$  octahedron. Peaks I at  $265\text{ cm}^{-1}$  is assigned to inter polyhedral Ta–O–Ta bending. The strong band J is attributed to Ta–Ta vibration.<sup>12,13</sup>

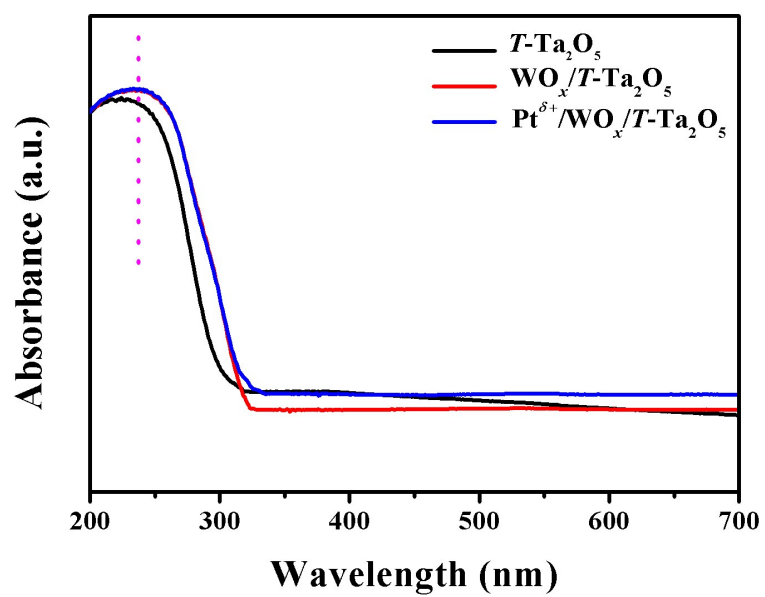


Figure S 3. UV-vis spectra of the as-synthesized catalysts.

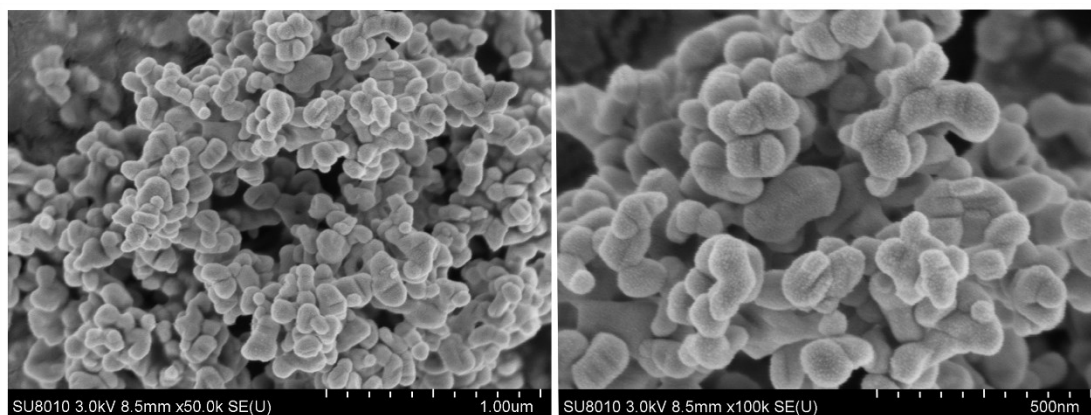


Figure S 4. SEM images of  $\text{Pt}^{\delta+}/\text{WO}_x/T\text{-Ta}_2\text{O}_5$ .

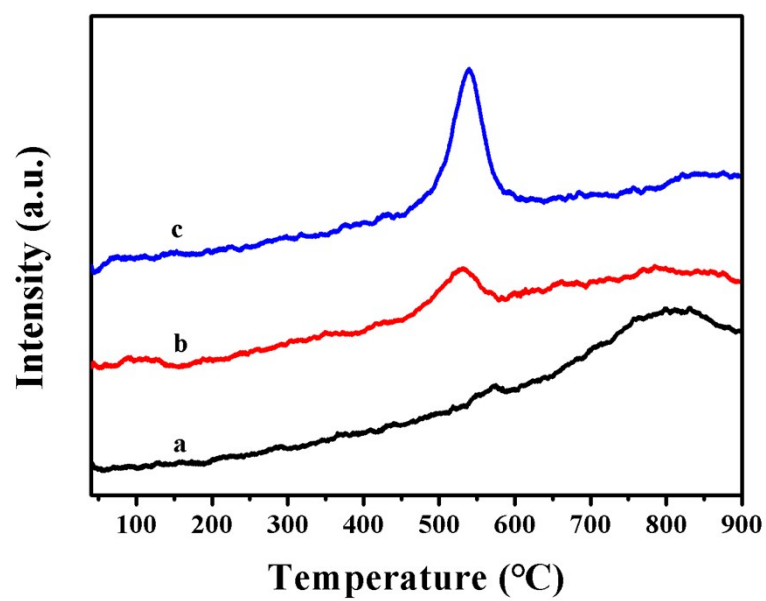


Figure S 5. H<sub>2</sub>-TPR profiles of WO<sub>x</sub>/T-Ta<sub>2</sub>O<sub>5</sub> (a), Pt/T-Ta<sub>2</sub>O<sub>5</sub> (b) and Pt<sup>6+</sup>/WO<sub>x</sub>/T-Ta<sub>2</sub>O<sub>5</sub> (c) catalysts.

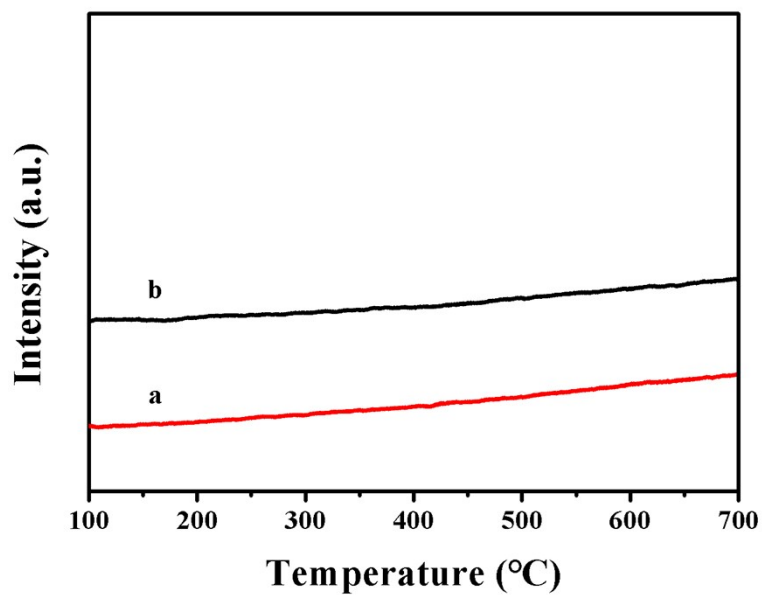
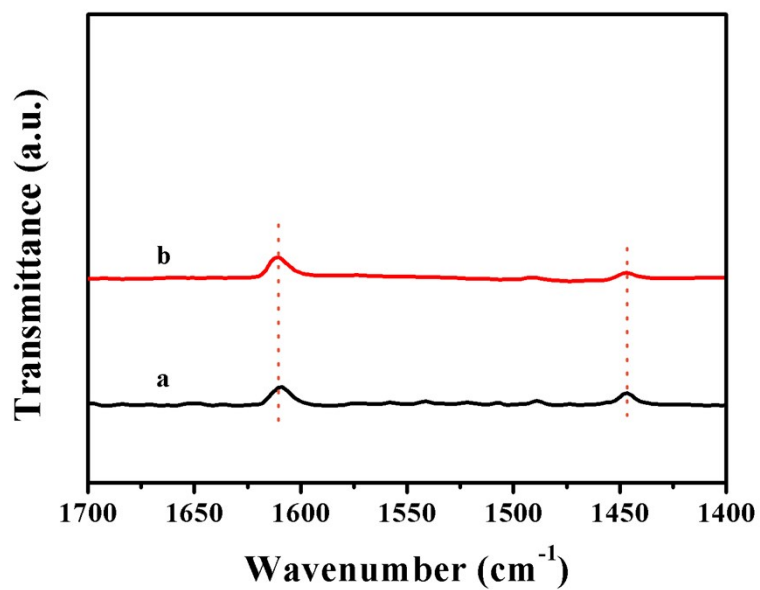
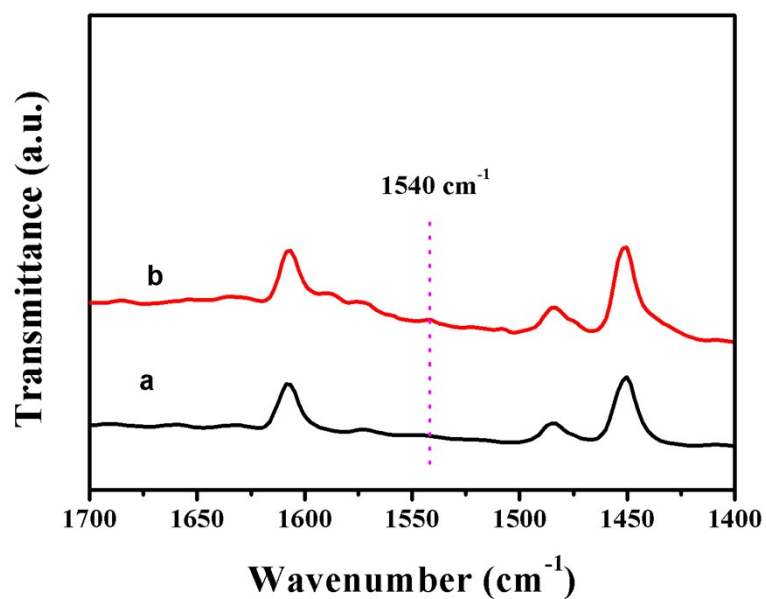


Figure S 6. NH<sub>3</sub>-TPD profiles of T-Ta<sub>2</sub>O<sub>5</sub> (a) and Pt<sup>6+</sup>/WO<sub>x</sub>/T-Ta<sub>2</sub>O<sub>5</sub> (b) catalysts.



**Figure S 7.** Py-IR profiles of  $T\text{-Ta}_2\text{O}_5$  (a) and  $\text{Pt}^{\delta+}/\text{WO}_x/T\text{-Ta}_2\text{O}_5$  (b) catalysts acquired at 573K.



**Figure S 8.** Py-IR spectra of the  $\text{Pt}^{\delta+}/\text{WO}_x/T\text{-Ta}_2\text{O}_5$  catalyst (a) and co-feeding  $\text{H}_2$  with pyridine (b) acquired at 373 K.

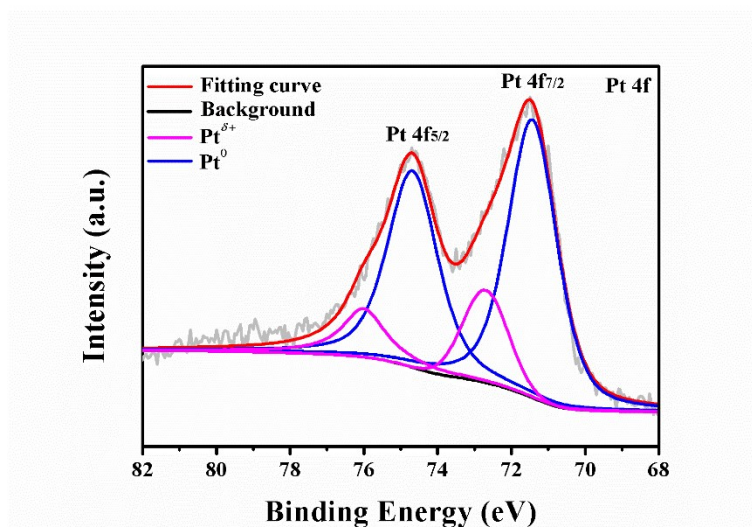


Figure S 9. XPS spectra for Pt 4f of Pt<sup>0</sup>/WO<sub>x</sub>/T-Ta<sub>2</sub>O<sub>5</sub> catalyst.

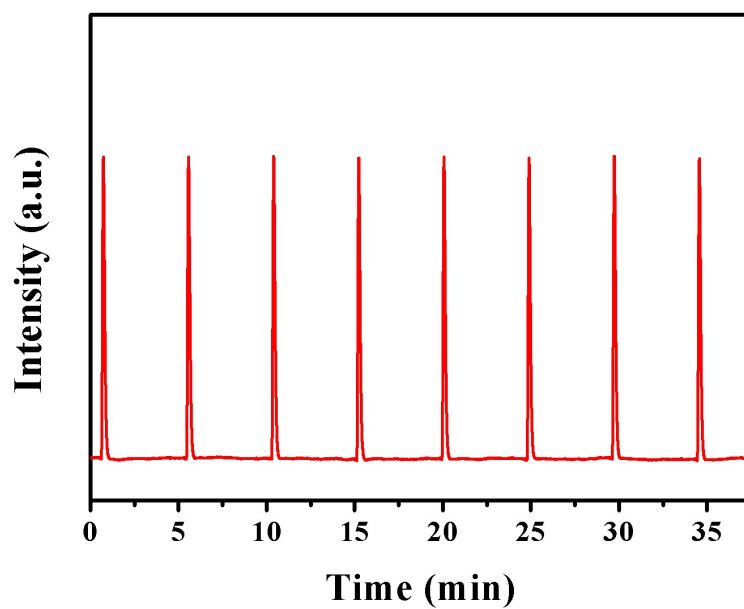


Figure S 10. H<sub>2</sub>-O<sub>2</sub> titration profiles for WO<sub>x</sub>/T-Ta<sub>2</sub>O<sub>5</sub>.

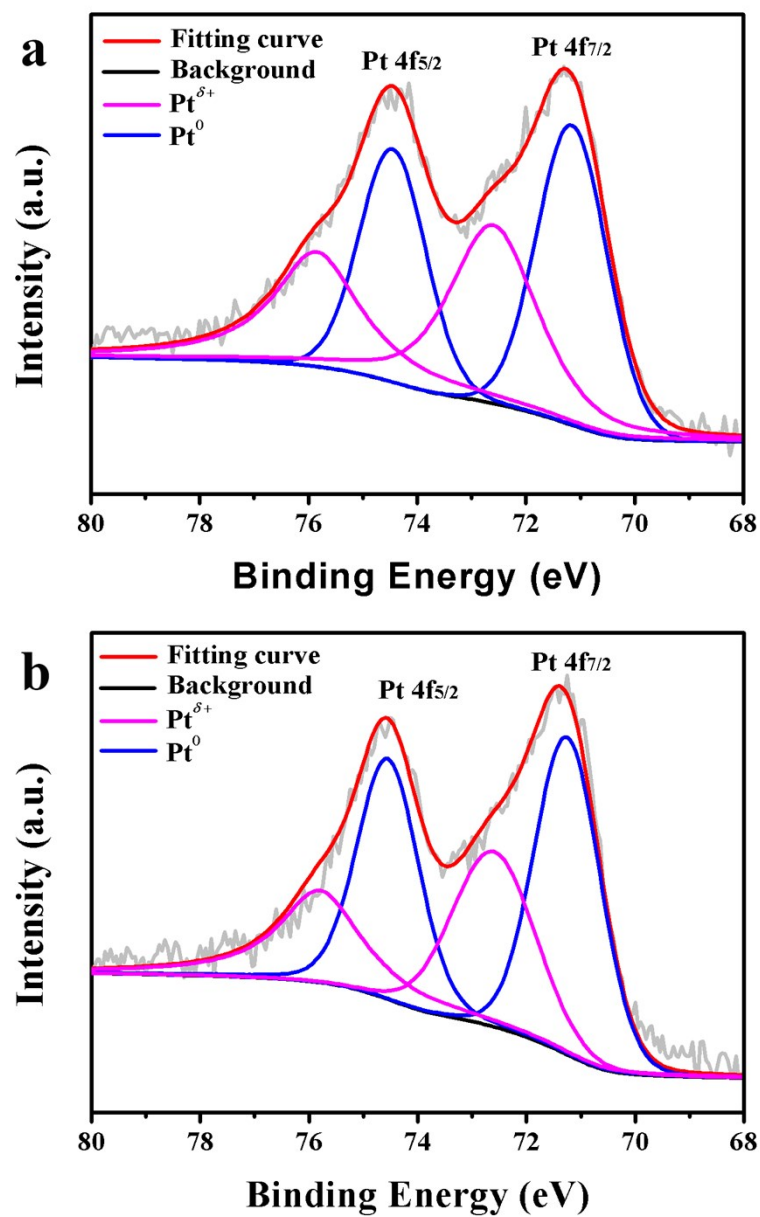


Figure S 11. XPS spectra for Pt 4f of Pt<sup>δ+</sup>/WO<sub>x</sub>/T-Ta<sub>2</sub>O<sub>5</sub> catalyst after 1st (a) and 4th (a) run, respectively.

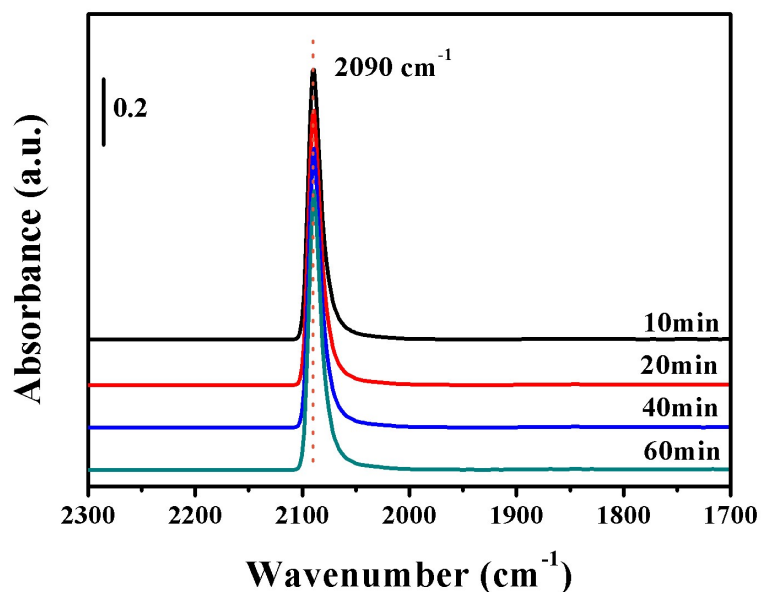


Figure S 12. IR spectra of CO adsorbed on Pt<sup>6+</sup>/WO<sub>x</sub>/T-Ta<sub>2</sub>O<sub>5</sub> catalyst after the 4th run.

#### Reference

- 1 T. Ushikubo and K. Wada, *Chem. Lett*, 1988, **17**, 1573–1574.
- 2 S. García-Fernández, I. Gandarias, J. Requies, M. B. Güemez, S. Bennici, A. Auroux and P. L. Arias, *J. Catal*, 2015, **323**, 65–75.
- 3 S. S. Priya, V. P. Kumar, M. L. Kantam, S. K. Bhargava, A. Srikanth and K. V. R. Chary, *Ind. Eng. Chem. Res*, 2015, **54**, 9104–9115.
- 4 S. Zhu, X. Gao, Y. Zhu and Y. Li, *J. Mol. Catal. A Chem*, 2015, **398**, 391–398.
- 5 R. Arundhathi, T. Mizugaki, T. Mitsudome, K. Jitsukawa and K. Kaneda, *ChemSusChem*, 2013, **6**, 1345–1347.
- 6 T. Kurosaka, H. Maruyama, I. Naribayashi and Y. Sasaki, *Catal. Commun*, 2008, **9**, 1360–1363.
- 7 S. Zhu, X. Gao, Y. Zhu, J. Cui, H. Zheng and Y. Li, *Appl. Catal. B Environ*, 2014, **158–159**, 391–399.
- 8 L. Gong, Y. Lu, Y. Ding, R. Lin, J. Li, W. Dong, T. Wang and W. Chen, *Appl. Catal. A Gen*, 2010, **390**, 119–126.
- 9 Y. Fan, S. Cheng, H. Wang, J. Tian, S. Xie, Y. Pei, M. Qiao and B. Zong, *Appl. Catal. B Environ*, 2017, **217**, 331–341.
- 10 W. Zhou, Y. Li, X. Wang, D. Yao, Y. Wang, S. Huang, W. Li, Y. Zhao, S. Wang and X. Ma, *J. Catal*, 2020, **388**, 154–163.
- 11 N. Lei, X. Zhao, B. Hou, M. Yang, M. Zhou, F. Liu, A. Wang and T. Zhang, *ChemCatChem*, 2019, **11**, 3903–3912.
- 12 U. Balachandran and N. G. Eror, *J. Mater. Sci. Lett*, 1982, **1**, 219–222.
- 13 T. Tsuchiya, H. Imai, S. Miyoshi, P. A. Glans, J. Guo and S. Yamaguchi, *Phys. Chem. Chem. Phys*, 2011, **13**, 17013–17018.